Arch Virol (2002) 147: 961–979
DOI 10.1007/s00705-001-0779-x

Archives of Virology
Printed in Austria

Exploitation of the Herpes simplex virus translocating protein VP22 to carry influenza virus proteins into cells for studies of apoptosis: direct confirmation that neuraminidase induces apoptosis and indications that other proteins may have a role*

S. J. Morris[1], **H. Smith**[2], and **C. Sweet**[1]

[1,2]School of Biosciences, The University of Birmingham, Birmingham, U.K.
[2]The Medical School, The University of Birmingham, Birmingham, U.K.

Received June 27, 2001; accepted December 10, 2001
Published online March 18, 2002

Summary. Previously, we have shown that apoptosis induced by influenza virus was inhibited by an anti-neuraminidase compound [4-guanidino-2, 3-dehydro-N-acetylneuraminic acid (GG167; Relenza; Zanamivir)], which does not enter cells, and acts at the attachment/entry phase of virus replication. Furthermore, a virulent virus, clone 7a, induced greater levels of apoptosis than the attenuated A/Fiji and had greater neuraminidase (NA) activity. To confirm more directly that NA induces apoptosis, the NA of clone 7a and A/Fiji was expressed fused to the Herpes simplex virus tegument coat protein VP22, transfected into HeLa cells and the level of apoptosis determined. VP22 translocates between cells via the medium thus allowing expressed proteins to transfer to a larger number of cells than those originally transfected.

Clone 7a NA fused to VP22 induced a significant level of apoptosis whereas A/Fiji NA/VP22 did not, confirming that NA activity is an important determinant of apoptosis acting during fusion protein translocation between cells. Furthermore, the induction of apoptosis was abrogated by antibody to transforming growth factor-β, which is activated by NA. This approach also showed that VP22/NS1 proteins of both clone 7a and A/Fiji induced apoptosis when expressed alone but inhibited double stranded RNA-induced apoptosis suggesting that this protein may have a dual mode of action. Also, the M1 and M2 proteins of both viruses induced apoptosis but their NP proteins did not.

*The nucleotide sequences of the M and NS genes of clone 7a and A/Fiji have been submitted to the EMBL nucleotide sequence database and designated the following accession numbers: clone 7a M, AJ298948; A/Fiji M, AJ298947; clone 7a NS, AJ298949; A/Fiji NS, AJ298950.

Introduction

Many viruses encode proteins which modulate the apoptotic response in infected cells. Simian virus-40, Epstein-Barr virus and vaccinia virus encode proteins which inhibit apoptosis, whereas the products of Human immunodeficiency virus type-1 and Human Parvovirus B19 virus induce apoptosis [8, 41]. Influenza virus induces apoptosis in a range of cell types including HeLa, Vero, MDCK and monocytes in vitro [9, 13, 20, 31, 37] and murine lung and lymphoid tissue in vivo [25]. The viral proteins and the mechanisms involved are not fully elucidated. However, apoptosis proceeds via the activation of caspase-3 and caspase-8. Fas, FADD and the double stranded (ds) RNA-activated protein kinase, PKR, may be important mediators of this pathway, but a Fas independent pathway may also exist [36, 38, 39].

The induction of apoptosis during infection may contribute to influenza virus pathogenicity. Apoptosis induced by infectious agents, unlike cell death during development, has been shown to be associated with an inflammatory response, as many of the pathways leading to apoptosis are involved in the processing or expression of inflammatory cytokines [32]. These include the activation of interleukin (IL)-1β converting enzyme (ICE; caspase 1) which processes pro-IL1β and pro-IL18 into their active forms [18] and the activation of NF-κB and NF-IL6, which regulate the expression of many cytokine genes [2, 42]. Interestingly, the ability of clone 7a and A/Fiji to induce apoptosis appears to correlate with the severity of disease observed in the ferret model [5, 31]. Therefore, understanding the mechanisms of influenza virus-induced apoptosis is important in pathogenicity studies and may reveal new targets for anti-viral drugs.

Neuraminidase (NA) has been shown, indirectly, to be involved in influenza virus-induced apoptosis because the latter was partially abrogated in the presence of three NA inhibitors [26]. The inhibitors had no effect when added after the viral attachment and entry phase showing that NA acts early in the replication cycle. NA activates latent TGF-β, a known inducer of apoptosis in epithelial cells [34]. Furthermore, influenza virus-induced apoptosis is partially abrogated in the presence of a TGF-β antibody. It has been suggested that TGF-β activated by influenza virus NA is responsible for the apoptosis of lymphocytes and thus lymphopenia during acute infection [28]. However, a direct relationship between NA, TGF-β and apoptosis has not been proved.

In this paper we report the use of a novel expression system to directly confirm the apoptosis inducing ability of NA and to demonstrate that it acts via TGF-β. We also investigate the role of other influenza virus proteins. The proteins were expressed fused to the Herpes simplex virus tegument coat protein VP22, which translocates from cell to cell through the media, thus ensuring a majority of cells contain the expressed fusion protein. In our hands, cells transfected with such constructs regularly show that approximately 15% of the cells are transfected whilst 75–80% of the cells contain the protein of interest.

Materials and methods

Cells and viruses

HeLa cells were maintained in growth medium [Eagles minimum essential medium (MEM) supplemented with 0.7% sodium bicarbonate, 10% newborn calf serum, 4 mM L-glutamine, 100 IU/ml penicillin and 100 μg/ml streptomycin (Gibco BRL)]. The virus strains, A/Fiji/15899/83 (H1N1) (A/Fiji) and clone 7a (H3N2) of the A/Puerto Rico/8/34 (H1N1) × A/England/939/69 (H3N2) reassortant system and the production of high titre virus stocks have been described previously [30].

Cloning of viral RNA segments

Virion RNA, extracted from high titre virus stocks using guanidinium isothiocyanate followed by isopropanol precipitation [11], was reverse transcribed with Superscript II RNase H^- (Gibco BRL) using a primer for the conserved 3′ untranslated region (UTR) found on all 8 segments (5′AGCAAAAGCAGG3′). This generated 8 cDNAs representing each of the 8 viral RNA segments. The cDNAs were then amplified using *Taq* polymerase and primers specific for the conserved 5′ (5′AGTAGAAACAAGG3′) and 3′ UTRs. Amplifications were performed as described previously [1]. Following purification by phenol:chloroform extraction and ethanol precipitation, the PCR products were shotgun cloned into a T-tailed vector, pVP22/*myc*-His-TOPO and Top10 competent cells using the pVP22 TOPO TA cloning kit version A (Invitrogen). The 5′ and 3′ termini of the inserted DNA were then sequenced using the Thermosequenase radiolabeled terminator cycle sequencing kit (Amersham) to confirm the identity of each clone. This generated pVP22-FPB2, pVP22-FNP, pVP22-FNA, pVP22-FM, pVP22-FNS containing A/Fiji PB2, NP, NA, M and NS genes respectively and pVP22-7aNP, pVP22-7aNA, pVP22-7aM, pVP22-7aNS containing clone 7a NP, NA, M and NS genes respectively.

Construction of the expression vectors

The pVP22/*myc*-His derived plasmids pSJM-FPB2, pSJM-FNP, pSJM-FNA, pSJM-FM1, pSJM-FNS1, pSJM-7aNP, pSJM-7aNA, pSJM-7aM1, pSJM-7aNS1 in which A/Fiji PB2, NP, NA, M1 and NS1 and clone 7a NP, NA, M1 and NS1 genes respectively, were cloned 'in frame' with VP22, were generated as follows. The open reading frame (ORF) of each gene was amplified by a standard PCR using the cloned virion segments as templates. Primers were designed to include the first and last coding residues of individual segments, so that the products generated would lack a start and stop codon. This allowed read through of the VP22 ORF, viral gene ORF and the *myc* & His tag, when cloned into the pVP22/*myc*-His-TOPO expression vector. Following purification by phenol:chloroform extraction and ethanol precipitation the PCR products were cloned directly into a pVP22/*myc*-His-TOPO vector as described previously. The inserted DNA was sequenced using the Thermosequenase radiolabeled terminator cycle sequencing kit (Amersham) to check that each gene had been inserted correctly.

Construction of vectors expressing the spliced M2 and NS2 products

The M and NS genes of clone 7a and A/Fiji were sequenced from pVP22-FM, pVP22-7aM, pVP22-FNS and pVP22-7aNS using an ABI PRISM automated gene sequencer with the PE Applied Biosystems four dye technology (Lark Technologies, Saffron Walden, U. K.). The genes were then excised from these plasmids and cloned into the *Kpn*I and *Xba*I sites of pGEM7Zf(+) (Promega). The ORF of M2 and NS2 was generated by inverse PCR using Vent polymerase (New England Biolabs) and primers designed based on the 3′ splice acceptor sites

(5′GCCTATCAGAAACGAATG3′ for M2 and 5′GACATACTAATGAGGATGTC3′ for NS2) and 5′ splice donor sites (5′GTTTCGACCTCGGTTAGA3′ for M2 and 5′CTGAAAGCTT GACACAGTG3′ for NS2). All amplifications were performed using a denaturation step at 94 °C for 1 min, an annealing step at 55 °C for 2 min and an extension step at 72 °C for 5 min, followed by a 10 min extension at 72 °C at the end of cycling. The PCR products were phosphorylated at the 5′ termini and then re-circularised using T4 DNA ligase. The resulting plasmids were propagated in DH5α cells. The ORF of M2 and NS2 were amplified by PCR as above and cloned into the vector pVP22/*myc*-His-TOPO to generate pSJM-FM2, pSJM-7aM2 and pSJM-FNS2, in which A/Fiji M2, clone 7a M2 and A/Fiji NS2 genes respectively were cloned 'in frame' with VP22. The inserted DNA was sequenced as outlined above to confirm that the relevant genes had been inserted correctly 'in frame' with the ORF of VP22 and *myc*.

Transfection

HeLa cells were seeded into a 24 well flat bottomed cell culture plate containing sterile 13 mm glass coverslips. Once 60–80% confluent, the monolayer was washed twice with transfection medium [Eagles MEM supplemented with 0.7% sodium bicarbonate (Gibco BRL)] and then 250 μl transfection medium was added. Pre-complex reactions were prepared by diluting 0.5 μg purified plasmid DNA and 4 μl PLUS reagent (Gibco BRL) in 25 μl transfection medium and incubating at room temperature for 15 min. 2.5 μl LipofectAMINE reagent (Gibco BRL) was diluted in 25 μl transfection medium before addition to the pre-complex reaction. After 15 min at room temperature, the DNA-PLUS-LipofectAMINE complexes were added to the medium overlaying the cells. Cells were incubated at 37 °C for 3 h and then 1 ml maintenance medium (growth medium with serum concentration reduced to 2%) added. The vector pVP22/*myc*-His (pVP22), a circularised form of pVP22/*myc*-His-TOPO, expressing VP22 alone, was used as a control vector in all transfection experiments.

Treatment of transfected cells with GG167

Cells were grown in 24 well cell culture plates and transfected as described above, except that after incubating the cells with the DNA-PLUS-LipofectAMINE complexes for 3 h, the medium was removed and replaced with maintenance medium alone or medium containing 500 μg/ml of the neuraminidase inhibitor 4-guanidino-2, 3-dehydro-N-acetylneuraminic acid (GG167, Relenza, Zanamivir), kindly supplied by R. Fenton, Glaxo Smithkline, Stevenage, U. K.

Treatment of transfected cells with anti-pan transforming growth factor-β antibody

Cells were grown in 24 well cell culture plates and transfected as described above, except that after incubating the cells with the DNA-PLUS-LipofectAMINE complexes for 3 h, the medium was removed and replaced with maintenance media alone or medium containing 33.3 μg/ml anti-pan transforming growth factor (TGF)-β antibody (Sigma).

Treatment of transfected cells with polyriboinosinic-polyribocytidylic acid

Cells were grown in 24 well cell culture plates and transfected as described above, except that after incubating the cells with the DNA-PLUS-LipofectAMINE complexes for 3 h, the medium was removed and replaced with maintenance media alone or medium containing 50 μg/ml polyriboinosinic-polyribocytidylic acid (polyI-C) (Sigma).

Cytotoxicity assays

Cytotoxicity assays were performed using the Cytotox 96 assay (Promega) as described previously [31].

PCR analysis of fusion protein expression

Transfected cells (from 4 wells) were harvested by scraping into phosphate buffered saline (Dulbecco's A; PBSA). Total cellular RNA, was extracted using guanidinium isothiocyanate followed by isopropanol precipitation. Any remaining DNA was removed from the RNA sample by adding RQ1 DNase (Promega) at a final concentration of 10 μg/ml. The sample was incubated for 15 min at 37 °C and then transferred to 70 °C for 15 min to heat inactivate the enzyme. Total cellular RNA was reverse transcribed with Superscript II RNase H^- (Gibco BRL) using the primers NS1 reverse (5′ATCAGCCATCTTATTTCTTCG3′), A/Fiji NA reverse (5′CTTGTCAATGGTGAATGGCAAC3′), clone 7a NA reverse (5′TATAGGCATGAA ATTGATGTCCG3′), or β-actin reverse (5′CTAGAAGCATTGCGGTGGACGATGGAG GG3′) [27]. The cDNA generated was then amplified using *Taq* polymerase to detect either β-actin, A/Fiji NS, A/Fiji NA, clone 7a NS1, and clone 7a NA mRNA synthesis using the reverse primers described above and the following forward primers: β-actin (5′TGACGGGGTC ACCCACACTGTGCCCATCTA3′), A/Fiji NS1 (5′TGGATCCCAACACTGTGT3′), clone 7a NS1 (5′TGGATCTAACACTGTGT3′), A/Fiji NA (5′TGAATCCAAATCAGAAAATA ATA3′), clone 7a NA (5′TGAATCCAAATCAAAATAGAATA3′). mRNA synthesis of A/Fiji M, A/Fiji NP, clone 7a M and clone 7a NP was analysed as above using the vector specific primers, pcDNA3 1/BGH reverse (5′TAGAAGGCACAGTCGAGG3′) (Invitrogen) and pVP22 forward (5′GGCCACGGCGACTCGA3′). A negative control reaction, containing no DNA was performed, as well as a positive control reaction using plasmid DNA as the template. All amplifications used a denaturation step at 94 °C for 1–2 min and an extension step at 72 °C for 1–2 min followed by a 10 min extension at 72 °C at the end of cycling. Viral gene specific amplifications used an annealing temperature of 53.5 °C for 2 min, whereas β-actin amplification required an annealing temperature of 72 °C for 45 sec.

Protein analysis using Western blotting

Transfected cells were washed once with PBSA and harvested by scraping into 1 ml PBSA followed by centrifugation at 1500 × **g** for 5 min. Cells were resuspended in 50 μl cell lysis buffer (50 mM Tris-HCl, pH7.8, 150 mM sodium chloride and 1% Nonidet P40) and incubated at 37 °C for 10 min. Cell nuclei were pelleted by centrifugation at 10, 000 × **g** for 10 min and the lysate, containing the proteins, retained. Protein samples were dried to completeness under vacuum and resuspended in 5–10 μl of 1 × SDS loading buffer. Proteins were concentrated through 4% SDS-polyacrylamide before being resolved through 8–12% SDS-polyacrylamide, using the Bio-Rad mini-protean system (Bio-Rad). A set of biotinylated broad range SDS-PAGE molecular weight standards (Bio-Rad), diluted 1:8, were run alongside the samples. After electrophoresis the proteins were transferred from the polyacrylamide gel to nitrocellulose membrane, Hybond-C (Amersham Pharmacia Biotech), electrophoretically, using a Blot Transfer Cell (Bio-Rad). The membrane was then incubated with blocker (0.1% sodium azide, 0.1% Tween-20 and 3% BSA in PBS) for 18 h, with gentle shaking. After blocking, the membrane was probed with either anti-*myc* mouse monoclonal antibody (Invitrogen), anti-VP22 polyclonal antibody, AGV-30, anti-NP monoclonal antibody raised against influenza virus X-31 (H3N2), anti-N1 polyclonal antibody raised against the H3N1 reasssortant influenza virus A/Memphis/102/72 (H3N2) × A/Bellamy/42 (H1N1) or anti-N2 polyclonal antibody raised against the H1N2 reassortant influenza virus A/NWS/33 (H1N1) × A/Tokyo/67 (H2N2). The antibodies were diluted in PAT with sodium azide (1%

BSA, 0.001% Tween-20 and 0.1% sodium azide in PBS). After 5 h of gentle shaking, the membrane was washed three times with PBS for 10 min each time and either horseradish peroxidase (HRP)-conjugated-rabbit-anti-mouse IgG (Dako) or HRP-conjugated-goat-anti-rabbit Ig (Dako), diluted 1:1000 in PAT, added. The membrane was incubated with secondary antibody for 1 h and then washed six times with PBS, for 5 min each time. After incubating with the antibodies the membrane was incubated with HRP-streptavidin (Amersham Pharmacia Biotech), diluted 1:1000 in PAT, for 1 h and then washed six times with PBS, for 5 min each time, to detect the biotinylated markers. The antigens were detected by enhanced chemiluminescence (ECL) using the ECL^{TM} Western Blotting Detection Reagents (Amersham Pharmacia Biotech).

Determination of the percentage of apoptotic and transfected cells by fluorescence microscopy

Cell monolayers, 24–48 h post transfection, were washed twice with PBSA and fixed with 100% methanol [4]. After 5 min at room temperature the cells were washed five times with PBSA and then incubated with PBSA containing 10% foetal calf serum (PBSAF) (blocking solution) for 30 min at room temperature, with gentle shaking. The blocking solution was removed and cells incubated with anti-*myc*-mouse monoclonal IgG1 antibody (Invitrogen), diluted 1:250 in PBSAF, for 1 h at room temperature. Cells were then washed three times with PBSA and incubated with FITC-conjugated-rabbit-anti-mouse IgG, diluted 1:250 in PBSAF, for a further hour at room temperature. After washing three times with PBSA, propidium iodide (1 μg/ml) was added and the cells incubated at 4 °C for 30 min. The cells were then washed three times with PBSA before the coverslips were mounted on to microscope slides, using triethylenediamine (DABCO), in alkaline buffered saline. Cells were visualised under ultraviolet light using a Zeiss microscope with an IV FI Epi-fluorescence condenser at a magnification of ×500. Apoptotic cells were distinguished from healthy cells by their fragmented nuclei. Transfected cells were distinguished by bright cytoplasmic FITC fluorescence. Cells that contained the fusion proteins due to translocation via the media had patchy cytoplasmic staining and/or dense nuclear staining [6, 7].

Analysis of fusion protein expression and location by confocal microscopy

Cell monolayers, 48 h post transfection, were washed twice with PBSA and fixed with 100% methanol [4]. After 5 min at room temperature the cells were washed five times with PBSA and then incubated with PBSAF for 30 min at room temperature, with gentle shaking. Blocking solution was removed and the cells were incubated for 1 h at room temperature with either a) anti-*myc*-mouse monoclonal IgG1 antibody (Invitrogen), diluted 1:250 in PBSAF, b) anti-VP22 polyclonal antibody, AGV-30, diluted 1:500 in PBSAF, c) anti-N1 polyclonal antibody raised against the H3N1 reassortant influenza virus A/Memphis/102/72 (H3N2) × A/Bellamy/42 (H1N1), diluted 1:1000 in PBSAF or d) anti-N2 polyclonal antibody raised against the H1N2 reassortant influenza virus A/NWS/33 (H1N1) × A/Tokyo/67 (H2N2), diluted 1:1000 in PBSAF. Cells were then washed three times with PBSA and incubated for a further hour at room temperature with FITC-conjugated-rabbit-anti-mouse IgG or FITC-conjugated-goat-anti-rabbit Ig respectively, diluted 1:250 in PBSAF. After washing three times with PBSA the coverslips were mounted on to microscope slides, using DABCO, in alkaline buffered saline.

Cells were analysed using the MRC-600 laser scanning confocal imaging system (Bio-Rad), with an argon ion laser (25 mwatt, 488 nm & 514 nm wavelength) coupled to a Nikon Diaphot 2 inverse ultraviolet microscope. Antigens conjugated to FITC were detected using the high sensitivity blue excitation filter set (BHS, 488 nm). Cells were viewed under

immersion oil, at a magnification of × 600. Images were collected using the MRC-600 confocal microscope operating software (coMOS), version 7.1 beta 2 (Bio-Rad), set for Kalman filtering (10 scans in total). They were then processed using Confocal Assistant, version 3.1.

Statistical analysis

Data was collated and analysed for statistical significance by the Student's t-test.

Results

Construction of the expression plasmids

Multiplex RT-PCR resulted in the amplification of all 8 RNA segments from clone 7a and A/Fiji. Shotgun cloning into a T-tailed vector, pVP22/*myc*-His-TOPO resulted in the generation of plasmids each containing a single viral gene, as confirmed by sequencing the 5′ and 3′ termini of the inserted DNA. This sequence data was used to design specific primers to amplify the ORF of the genes, which were then cloned into the pVP22/*myc*-His-TOPO vector. Although the ORF from all the genes of both viruses were successfully amplified, plasmids containing clone 7a and A/Fiji PB1, PA and HA ORFs and clone 7a PB2 ORF could not be identified. This may be due to the toxic nature of the gene product expressed from a putative prokaryotic promoter present in the vector (personal communication M. Brodie, Invitrogen).

The cloned NA, M1, M2, NS1 and NS2 ORFs from both viruses were fully sequenced to check for random point mutations generated during amplification. Although several base substitutions were identified in all the sequences, in all but one case, these mutations did not alter the peptide sequence. The NS1 gene sequence from A/Fiji contained an A to T point mutation at position 392 generating a stop codon in the encoded peptide, which would result in the synthesis of an NS1 protein containing the N-terminal 130 amino acids only. This plasmid was designated pSJM-FNS1del and another plasmid was generated which encoded the full-length NS1 protein.

Fusion protein expression was checked by immunofluorescence, with anti-VP22, anti-*myc* and, in the case of the NA fusion proteins, anti-N1 and anti-N2 influenza virus specific antibodies; mRNA synthesis was also analysed. A typical example of mRNA analysis is shown in Fig. 1. RT-PCR amplification products of similar size to that amplified in the positive control reactions containing either pSJM-7aNS1 (890 bp) or pSJM-7aNA (1450 bp) were detected from the total cellular RNA of cells transfected with either pSJM-FNS1, pSJM-7aNS1, pSJM-FNA or pSJM-7aNA (Fig. 1a). β-actin (661 bp) was reverse transcribed and amplified as a control to check the quality of the RNA obtained from mock and pVP22 transfected cells (Fig. 1b).

Clone 7a and A/Fiji NA VP22 fusion proteins induce different levels of apoptosis

The level of apoptosis was examined in HeLa cells transfected with pVP22, pSJM-FNA or pSJM-7aNA 48 h post transfection (Table 1). The level of apoptosis

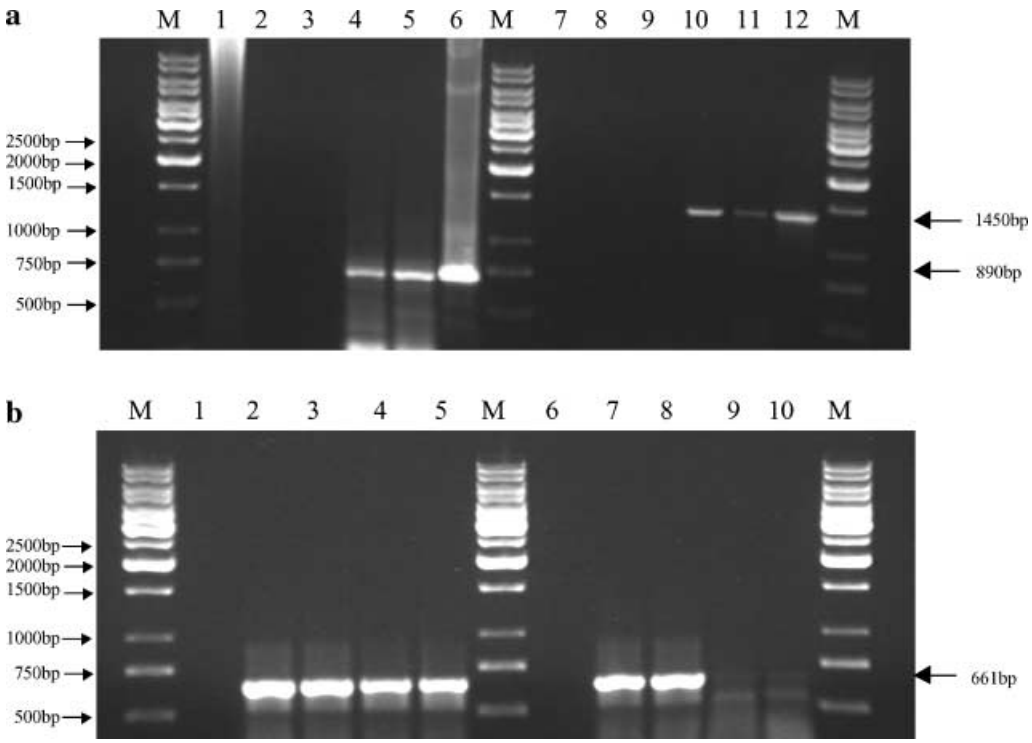

Fig. 1. Analysis of mRNA from cells transfected with either pSJM-FNS1, pSJM-7aNS1, pSJM-FNA or pSJM-7aNA. Total RNA was extracted from transfected cells and the specific fusion protein mRNA amplified by RT-PCR using **a** influenza virus gene specific primers. *M* marker (1 kb ladder; MBI Fermentas); *1*, *7* negative PCR control; *2*, *8* mock transfected cells; *3*, *9* cells transfected with pVP22; *4* cells transfected with pSJM-FNS1; *5* cells transfected with pSJM-7aNS1; *6* positive PCR control using pSJM-7aNS1 as the template DNA; *10* cells transfected with pSJM-FNA; *11* cells transfected with pSJM-7aNA; *12* positive PCR control using pSJM-7aNA as the template DNA; **b** β-actin specific primers. *M* Marker (1 kb ladder; MBI Fermentas); *1*, *6* negative PCR control; *2*, *7* mock transfected cells; *3*, *8* cells transfected with pVP22; *4* cells transfected with pSJM-FNS1; *5* cells transfected with pSJM-7aNS1; *9* cells transfected with pSJM-FNA; *10* cells transfected with pSJM-7aNA. All RT-PCR products were resolved through 0.7% agarose containing ethidium bromide and visualised under UV light

induced varied between experiments, but in each experiment the fusion protein VP22-A/Fiji NA (VP22FNA) did not induce a significant ($P > 0.5$) level of apoptosis when compared to that induced by VP22 alone. In contrast, VP22-clone7a NA (VP227aNA) induced a significantly greater level of apoptosis than both VP22 ($P < 0.001$) and VP22FNA ($P < 0.001$).

The average level of cytotoxicity (a measure of cell lysis due to the transfection procedure and late apoptosis) detected for cells transfected with pSJM-FNA was similar to that obtained for cells transfected with pVP22 (Table 1). Therefore, the low number of apoptotic cells present on the monolayer at 48 h post transfection is not due to the lysis of cells during the late stages of apoptosis in vitro. The level of cytotoxicity generated by the expression of VP227aNA was significantly greater

Table 1. Level of apoptosis and cytotoxicity induced 48 h post transfection by the expression of VP22 alone and by expression of VP22 clone 7a and A/Fiji NA fusion proteins

Experiment[c]	% Cells showing apoptosis (±SD)[a]			% Cytotoxicity (±SD)[b]		
	VP22	VP22FNA	VP227aNA	VP22	VP22FNA	VP227aNA
1	10.7 (3.3)	9.4 (1.5)	19.9 (1.6)	17.5 (4.0)	12.7 (2.8)	23.5 (0.5)
2	8.7 (2.0)	9.3 (2.4)	22.6 (3.7)	16.0 (1.0)	12.8 (1.1)	32.9 (3.5)
3	8.1 (2.5)	10.5 (1.8)	25.8 (2.1)	10.2 (0.9)	7.2 (2.8)	19.6 (0.0)

[a]Apoptotic cells were determined on the basis of nuclear morphology (as described in Materials and methods). The percentage of apoptotic cells was calculated as a percentage of the total number of cells counted (approx. 1000 for each sample)

[b]Cytotoxicity was determined by the release of lactate dehydrogenase (LDH) from cells whose plasma membrane integrity has been lost. Percentage cytotoxicity was calculated as a percentage of LDH liberated from fully lysed cells

[c]All constructs were directly compared in these 3 experiments. The results are typical of 4–8 additional tests for each construct determined individually or in comparisons with constructs expressing different proteins

($P < 0.05$) than that detected for VP22 and VP22FNA in all experiments. This suggests that the number of apoptotic cells present on the coverslips at 48 h post transfection is actually an underestimate for cells expressing VP227aNA. The level of transfection was similar for all three constructs (approximately 16%) but the fusion proteins were detected in greater than 80% of cells due to translocation mediated by the VP22 moiety. We cannot, at this time, rule out the possibility that the difference in ability of clone 7a and A/Fiji NA to induce apoptosis may be due to differential expression of the two fusion proteins, as attempts to quantify the level of expression of VP22FNA and VP227aNA by western blotting were unsuccessful (data not shown).

Location of VP22FNA and VP227aNA

Laser scanning confocal microscopy showed a distinct staining pattern for both fusion proteins when stained with the anti-VP22 antibody (Fig. 2). This pattern was similar when cells were stained using the anti-myc antibody (data not shown). Hence, the proteins synthesised must have contained VP22 fused to the viral protein with the *myc* epitope at the C-terminus. In addition, anti-N1 and anti-N2 antibodies detected VP22FNA (Fig. 2k) and VP227aNA (Fig. 2n) respectively providing further evidence for the expression of these proteins. Mock transfected cells showed little or no fluorescence with either the anti-VP22 (Fig. 2a), anti-N1 (Fig. 2i) or anti-N2 (Fig. 2l) antibodies indicating high specificity of the antibodies for their respective fusion proteins.

VP22 is expressed in the cytoplasm of transfected cells (Fig. 2b), except when the cell is undergoing mitosis, but translocates to the nucleus of recipient cells (Fig. 2c) [6]. This distribution pattern is evident in cells stained with the anti-VP22 antibody (Fig. 2b and c).

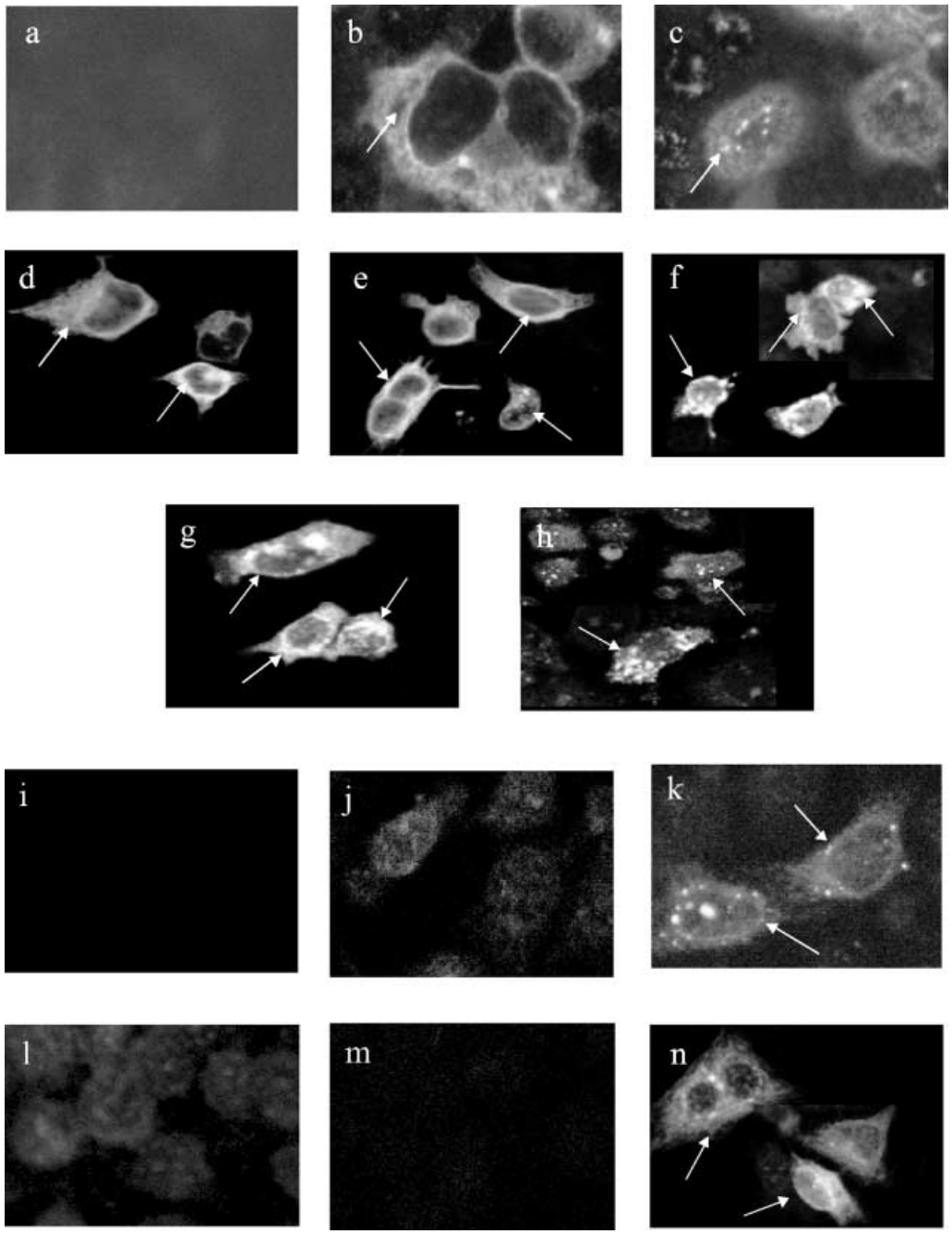

Fig. 2. Location of A/Fiji NA and NS1 and clone 7a NA and NS1 fusion proteins. Cells were stained with either rabbit anti-VP22 antibody (**a**–**h**), rabbit anti-N1 antibody (**i**–**k**) or rabbit anti-N2 antibody (**l**–**n**), followed by FITC labelled goat-anti-rabbit antibody, 48 h post-transfection (**a**, **i**, **l**) or transfection with control plasmid pVP22/*myc*-His (**b**, **c**, **j**, **m**), pSJM-FNA (**d**, **k**), pSJM-7aNA (**e**, **n**), pSJM-FNS1 (**f**), pSJM-7aNS1 (**g**) or with pSJM-FNS1del (**h**). Images were taken using the MRC-600 laser scanning confocal imaging system with an argon ion laser and BHS filter set at a magnification of $\times 600$. Images were collected using the coMOS software and manipulated using the confocal assistant package. Transfected cells showing predominately cytoplasmic staining are indicated by arrows whereas cells containing translocated fusion protein are indicated with arrowheads

VP22FNA and VP227aNA were predominantly located in the cytoplasm of most cells. Cells expressing VP22FNA showed diffuse cytoplasmic staining (Fig. 2d and k). The pattern observed is highly filamentous under higher magnification, which may represent an actin cytoskeleton; the ability of VP22 to bind to actin is a fundamental aspect of its ability to translocate between cells [6]. This staining pattern was also observed to some extent in cells expressing VP22 alone (Fig. 2b). Cells containing translocated VP22FNA predominantly showed perinuclear staining (Fig. 2d and k). The latter was more evident when anti-*myc* antibody was used (data not shown) but this may reflect the binding of this antibody to cellular Myc proteins. Also, any faint nuclear staining with the anti-VP22 antibody may have been lost during imaging.

The VP227aNA pattern of staining is similar to that seen with VP22FNA (Fig. 2e and n). The presence of VP227aNA in the nucleus of cells could explain its induction of apoptosis, as this is an inappropriate location. In virus infected cells, NA is synthesised in the ER and locates to the plasma membrane [14]. However, immunofluorescence studies indicate that VP22FNA is also present in this location. Since, VP22FNA does not induce apoptosis, other factors must be involved in the induction of apoptosis by VP227aNA.

GG167 inhibits VP227aNA induced apoptosis

Transfected cells were treated with 500 μg/ml GG167 and cells analysed for apoptosis 24 h post transfection. Table 2a shows the results obtained from 2 of 3 experiments. VP227aNA induced a significantly ($P < 0.05$) lower level of apoptosis in the presence of GG167 compared to that induced when GG167 was absent. GG167 had no significant effect on the level of apoptosis induced by VP22 or VP22FNA. These results showing that NA activity is essential for the induction of apoptosis by VP227aNA agree with previous results using infected MDCK cells [26].

Anti-TGF-β antibody inhibits VP227aNA-induced apoptosis

Treatment of cells, expressing VP22, VP22FNA or VP227aNA, with anti-pan-TGF-β antibody inhibited the induction of apoptosis by VP227aNA but had no effect on the level of apoptosis induced by VP22 or VP22FNA (Table 2b). The observation that VP227aNA induced apoptosis is mediated by TGF-β is in agreement with previous reports [28, 34].

VP227aNS1 and VP22FNS1 proteins induce apoptosis

HeLa cells transfected with pVP22, pSJM-FNS1, pSJM-7aNS1 or pSJM-FNS1del were analysed for apoptosis 48 h post transfection. The level of apoptosis induced by VP22FNS1, VP227aNS1 and VP22FNS1del was significantly ($P < 0.01$) greater than that induced by VP22 alone (Table 3). However, the levels of apoptosis induced by VP22FNS1 and the truncated fusion protein VP22FNS1del were not significantly ($P > 0.1$) different.

Table 2. Level of apoptosis induced by VP22, VP22FNA and VP227aNA in the presence or absence of **a** GG167 and **b** anti-pan-TGF-β antibody

Protein	Treatment[a]	% Cells showing apoptosis (±SD)[b]	
		Experiment 1	Experiment 2
a			
None	−	1.2 (0.5)	0.5 (0.3)
	+	1.3 (0.5)	1.5 (0.4)
VP22	−	3.9 (1.2)	6.8 (2.3)
	+	3.8 (1.1)	8.8 (2.9)
VP22FNA	−	5.3 (1.2)	6.6 (1.4)
	+	5.2 (1.2)	6.6 (1.2)
VP227aNA	−	14.2 (2.5)	12.8 (2.7)
	+	9.5 (1.8)	8.8 (2.1)
b			
None	−	1.5 (1.0)	1.9 (0.4)
	+	1.9 (1.0)	1.7 (0.6)
VP22	−	5.4 (0.6)	9.1 (2.1)
	+	4.9 (0.6)	11.2 (2.4)
VP22FNA	−	5.8 (0.6)	6.0 (1.8)
	+	5.7 (0.9)	4.7 (1.1)
VP227aNA	−	11.8 (2.5)	20.6 (6.7)
	+	6.8 (1.7)	12.4 (4.1)

[a]Cells were incubated with (+) or without (−) 500 μg/ml GG167 (a) or 33.3 μg/ml anti-pan-TGF-β antibody (b) from 3 h post transfection. Cells were analysed 24 h post transfection

[b]Apoptotic cells were determined on the basis of changes in nuclear morphology observed by staining with propidium iodide. The percentage is based on the total number of cells counted (approximately 1000 per sample)

Table 3. Level of apoptosis induced 48 h post transfection by the expression of the VP22NS1 fusion proteins of clone 7a and A/Fiji and the C-terminal deletion mutant of A/Fiji NS1 (VP22NS1del)

Experiment[b]	% Cells showing apoptosis (±SD)[a]			
	VP22	VP22FNS1	VP227aNS1	VP22FNS1del
1	6.2 (1.3)	15.1 (1.8)	14.8 (4.1)	14.0 (1.4)
2	11.8 (1.2)	16.9 (3.0)	21.2 (4.3)	17.8 (2.6)
3	12.6 (1.4)	19.8 (3.0)	23.0 (5.1)	20.3 (5.3)

[a]Apoptotic cells were determined on the basis of nuclear morphology (as described in Materials and methods). The percentage was calculated on the basis of the total number of cells counted (approx. 1000 for each sample)

[b]All constructs were directly compared in these 3 experiments. The results are typical of 4–8 additional tests for each construct determined individually or in comparisons with constructs expressing different proteins

VP22FNS1 was located predominantly in the cytoplasm of transfected cells, however faint nuclear staining was also evident (Fig. 2f); recipient cells showed perinuclear staining (Fig. 2f). This pattern of staining was also observed for VP227aNS1 (Fig. 2g). Cells expressing VP22FNS1del also showed cytoplasmic staining with the anti-VP22 antibody (Fig. 2h), although this was patchy compared to that seen for the other proteins. Cells containing translocated VP22FNS1del showed discrete nuclear staining (Fig. 2h). Therefore, the location of all three proteins resembled that expected during influenza virus infection [19].

VP22NS1 proteins from clone 7a and A/Fiji inhibit dsRNA-induced apoptosis

Our results and those published by Schultz-Cherry and colleagues [33, 35] suggest that NS1 induces apoptosis. However, others consider that the primary role of NS1 is to inhibit PKR and consequently apoptosis [3]. To investigate this further, cells expressing VP227aNS1 and VP22FNS1 were treated with the dsRNA homologue polyI-C and analysed for apoptosis 24 h post transfection (Table 4). In all experiments the level of apoptosis observed for the fusion proteins was significantly ($P < 0.05$) lower than that detected with either cells treated with polyI-C alone or VP22 transfected cells treated with polyI-C. The truncated form of A/Fiji NS1 (VP22FNS1del), which retains its RNA binding ability [22] also inhibited

Table 4. Level of apoptosis induced by VP22NS1 fusion proteins of clone 7a and A/Fiji in the presence of polyI-C

Protein	Treatment[a]	% Cells showing apoptosis (±SD)[b] in experiment			
		1	2	3	4
None	−	1.9 (0.8)	0.8 (0.3)	1.8 (1.1)	1.7 (0.4)
	+	25.6 (4.6)	32.4 (5.7)	42.3 (3.3)	30.6 (5.9)
VP22	−	9.4 (1.6)	8.5 (1.4)	9.6 (2.2)	8.4 (2.3)
	+	38.2 (6.9)	37.0 (5.1)	52.8 (9.0)	32.3 (4.9)
VP22FNS1	−	12.4 (1.9)	10.4 (0.7)	15.6 (3.0)	15.1 (4.2)
	+	19.2 (5.1)	29.3 (5.0)	21.9 (4.3)	16.9 (6.2)
VP227aNS1	−	11.8 (1.1)	14.5 (3.1)	27.5 (5.8)	18.4 (3.2)
	+	16.4 (3.7)	22.3 (2.8)	26.2 (5.6)	13.5 (3.8)
VP22FNS1del	−	ND	ND	12.0 (2.2)	15.0 (4.5)
	+	ND	ND	30.3 (6.1)	19.9 (5.5)

[a] Cells were incubated with (+) or without (−) 50 μg/ml polyI-C from 3 h post transfection and apoptosis quantified 24 h post transfection

[b] Apoptotic cells were determined on the basis of changes in nuclear morphology observed by staining with propidium iodide. The percentage was determined on the basis of the total number of cells counted (approximately 1000 per sample)

ND Not determined

dsRNA-induced apoptosis (Table 4). No difference between the level of transfection or translocation was observed in cells treated with or without polyI-C. Therefore, the inhibition of apoptosis in the presence of polyI-C was not due to sequestration of NS1 in transfected cells.

The effect of other viral fusion proteins on apoptosis

Both VP22FM1 and VP227aM1 induced a significant ($P < 0.01$) level of apoptosis compared to VP22 alone, as did the fusion proteins VP22FM2, VP227aM2 and VP22FNS2 (Table 5). Confocal microscopy, using either anti-VP22 antibody or anti-*myc* antibody, showed that VP22FM1 and VP227aM1 are present both in the nucleus and cytoplasm of most cells (data not shown). In contrast, VP22FM2 and VP227aM2 were predominantly located in the cytoplasm of both transfected and surrounding cells, but faint nuclear staining was also evident (data not shown). In addition, VP227aM2 exhibited some discrete, bright staining in the cytoplasm, which was not observed for VP22FM2 (data not shown). VP22FNS2 was located in the nucleus and in discrete locations around the nuclear envelope (data not shown). The location of all these chimaeric proteins reflects that seen during influenza virus infection [19]. Expression of VP22FM1 and VP227aM1 was also shown indirectly by mRNA synthesis (data not shown).

VP22FPB2 protein did not induce apoptosis [the average level induced by VP22FPB2 from 3 experiments was 11.8% (SD $\pm$ 2.6) compared to 10.5% (SD $\pm$ 2.2) for VP22], even though this protein was located in the nucleus of most cells as found during influenza virus infection [19]. The level of cytotoxicity generated by VP22FPB2 was similar to that detected for VP22 expression.

Clone 7a and A/Fiji VP22NP proteins induced a slightly greater level of apoptosis than VP22 alone [the average level of apoptosis induced was 12.1% (SD $\pm$ 1.6, n = 3), 11.2% (SD $\pm$ 2.4, n = 3) and 9.0% (SD $\pm$ 0.6, n = 3) for VP227aNP, VP22FNP and VP22 respectively]. However, the differences were

Table 5. Level of apoptosis induced 48 h post transfection by VP22M fusion proteins of clone 7a and A/Fiji and by the VP22NS2 fusion protein of A/Fiji

Experiment[b]	% Cells showing apoptosis ($\pm$SD)[a]					
	VP22	VP22FM1	VP227aM1	VP22FM2	VP227aM2	VP22FNS2
1	8.7 (1.0)	16.1 (3.4)	17.0 (2.0)	15.7 (3.2)	23.0 (3.1)	22.2 (0.7)
2	10.3 (1.9)	20.5 (4.4)	14.7 (3.0)	28.2 (4.4)	20.7 (3.5)	25.9 (2.0)
3	8.3 (1.8)	16.5 (0.8)	11.4 (1.2)	18.9 (3.9)	16.8 (2.4)	23.4 (2.7)

[a]Apoptotic cells were determined on the basis of nuclear morphology (as described in Materials and methods). The percentage was calculated on the basis of the total number of cells counted (approx. 1000 for each sample)

[b]All constructs were directly compared in these 3 experiments. The results are typical of 4–8 additional tests for each construct determined individually or in comparisons with constructs expressing different proteins

not significant ($P > 0.05$) in 3 out of 5 experiments for VP22FNP and 2 out of 3 experiments for VP227aNP. VP22FNP and VP227aNP were located both in the nucleus and cytoplasm of most cells (data not shown), thus reflecting the location of NP during infection [19]. VP22FNP and VP227aNP mRNA synthesis was also detected (data not shown).

Discussion

This is the first use of vector, pVP22/*myc*-His, to analyse the apoptosis inducing ability of influenza virus proteins. Previously, several non-influenza virus proteins had been fused to VP22 and translocation observed [6, 29]. One, p53, known to be involved in regulation of apoptosis, retained its ability to induce apoptosis [29]. This was therefore a valid system to use for the influenza virus proteins. It also provided a novel way of delivering the proteins to many cells, regardless of the level of transfection.

The overall conclusion from the results is that no single influenza virus protein is responsible for apoptosis. Indeed, several viral proteins induce apoptosis when expressed as a VP22 fusion protein, although, the relevance of these observations to influenza virus infection is unclear at present. The NA, M1, M2 and NS1 proteins from clone 7a and the M1, M2, NS1 and NS2 proteins from A/Fiji induced apoptosis while clone 7a and A/Fiji NP and A/Fiji PB2 and NA did not (Tables 1, 3 and 5). Although the differences in apoptosis observed were small, they were, in most cases, significantly greater than that seen with VP22 alone. In addition, these differences were consistently observed over numerous experiments. Further evidence to support the validity of these differences is the observation that NS1 induces apoptosis in other systems [33]. The results presented here indicate that influenza virus-induced apoptosis probably results from a combination of the effects of several proteins, which disrupt the finely tuned balance between pro- and anti-apoptotic host functions within the infected cell and inaugurates apoptosis. Some proteins may be apoptotic in some virus strains but not in others, e.g. the PB2 from A/WSN/33 appeared in preliminary experiments to be apoptotic unlike that from A/Fiji. Interestingly, Katze and colleagues have studied the H5N1 influenza viruses isolated from humans during the recent outbreak in Hong Kong; they found that the highly pathogenic viruses caused severe lymphopenia and apoptosis in the spleen and lungs of infected mice [17]. The pathogenic nature of these viruses was found to be associated with the NA, PB1, PB2 and M1 proteins [17]. In another study, overexpression of HA, M and NP as single proteins has been linked to the activation of NF-κB [10], a transcription factor involved in the regulation of many pro- and anti-apoptotic genes [16].

That viral proteins, not the VP22 moiety, were responsible for the observed apoptotic effects was indicated by the inhibition of VP227aNA-induced apoptosis by GG167 (Table 2a) and dsRNA-induced apoptosis by NS1 (Table 4). Apoptosis induction is not a function of the size of the expression vector or fusion proteins as the largest protein, VP22FPB2, did not induce apoptosis, however the smaller fusion proteins did. All the proteins could be detected by immunofluorescence

using either the anti-*myc* antibody to detect the C-terminal *myc* epitope (except VP22FNS1del, which does not contain the myc epitope), or the anti-VP22 antibody to detect the N-terminal VP22 moiety, i.e. the whole protein was synthesised. In addition, VP22FNA and VP227aNA were detected using anti-N1 and anti-N2 antibodies. Furthermore, the locations of the fusion proteins in general reflected that seen during infection.

The results provide direct evidence that NA is a major factor in the induction of apoptosis. Previous results had shown that clone 7a virus produced more apoptosis than A/Fiji, the apoptosis could be inhibited by GG167 [26, 30] and the NA of clone 7a was also more active than that of A/Fiji [26]. In the present work using fusion proteins, clone 7a NA had much greater apoptosis-inducing activity than A/Fiji NA. Furthermore, the inhibitory effect of GG167 on VP227aNA-induced apoptosis suggests that 7aNA activity is directly involved in the induction of apoptosis (Table 2a). Also, the inhibitory action of anti-TGF-β neutralising antibody (Table 2b) implicates activation of TGF-β in induction of apoptosis by 7aNA as shown in virus infected cells [24]. TGF-β is secreted from the cell and stored in the extracellular matrix in an inactive form [23]. Therefore, the activation of TGF-β by VP227aNA probably occurs during the translocation of VP227aNA from cell to cell and thus mimics events noticed previously during influenza virus attachment and entry [26]. This is supported by the fact that GG167 does not enter cells [26]. The subcellular location of the NA fusion proteins did not appear to affect apoptosis induction.

The inability of VP22FNA to induce apoptosis may be either connected to its low enzymatic activity compared to clone 7a or differences in the enzyme specificity of the NA from clone 7a and A/Fiji [26]. Alternatively, VP22FNA may be expressed at a lower level than VP227aNA, but this was not evident from the intensity of the immunofluorescence. Attempts to quantify the level of expression of VP22FNA and VP227aNA by western blotting were unsuccessful with the antibodies available, however NA from whole virus preparations was consistently detected using this technique. The gels suggested that the polyclonal antibodies were binding non-specifically to cellular proteins, that migrated to a similar position to the fusion proteins, masking the weak signal of the latter. The data obtained from the NA sequences of pSJM-7aNA and pSJM-FNA revealed several differences from the viral gene sequence reported previously [26], but these did not alter the peptide sequence, and no significant differences were evident for the residues comprising the enzyme active site between the strains.

VP227aNS1 and VP22FNS1 induced apoptosis when expressed alone (Tables 3 and 4) as previously reported for cells expressing NS1 under the control of a tetracycline repressor [33, 35]. In addition, VP22FNS1del, containing the N-terminal 130 amino acids only, induced apoptosis indicating that the C-terminal effector domain of NS1 is not required for this activity. This implies that inhibition of cellular mRNA polyadenylation is not responsible for the induction of apoptosis by these proteins. That VP22FNS1del is active agrees with a previous report that NS1 proteins containing mutations in the N-terminal RNA binding domain (residues 19–38) do not induce apoptosis [33]. Interestingly,

dsRNA-induced apoptosis was inhibited in cells expressing VP227aNS1, VP22FNS1 or VP22FNS1del (Table 4). This supports the view that NS1 inhibits PKR either by the sequestration of dsRNA [12, 21] or by direct interaction with PKR [40]. Hence, the induction of apoptosis by NS1 may be due to accumulation of NS1, which would not occur in the presence of dsRNA and consequently may not occur in virus infected cells. However, the pro-apoptotic activity of NS1 during influenza virus infection cannot be ruled out. Even though apoptosis induced by dsRNA was inhibited by the fusion proteins, the level of apoptosis observed did not decrease to the level seen when VP22 was expressed alone, in the absence of dsRNA (polyI-C). It appears that NS1 may possess both anti- and pro-apoptotic activities, which are modulated by other viral or cellular proteins during infection.

The experiment performed with dsRNA (polyI-C) emphasises the importance of investigating the effect of the viral proteins in a situation resembling infection where their apoptosis-inducing activities could be modulated by other cellular or viral proteins, as complex interactions occur during the replication cycle. Therefore, we are currently examining the apoptosis inducing ability of recombinant viruses, generated from cloned DNA, containing specific gene constellations from clone 7a and A/Fiji [15].

Acknowledgements

We would like to thank Dr. Rob Fenton and Dr. Richard Bethell at Glaxo Smithkline, Stevenage for providing the neuraminidase inhibitor, GG167, and Dr. K. May at the Marie Curie Research Institute, London, for providing the anti-VP22 antibody, AGV-30. We would also like to thank Dr. Jennifer McKimm-Breschkin at the Commonwealth Scientific and Industrial Research Organisation, Parkville, Victoria, Australia for providing the anti-N1 and anti-N2 antibodies. S. J. M. was supported by a studentship from the BBSRC.

References

1. Adeyefa CAO, Quayle K, McCauley JW (1994) A rapid method for the analysis of influenza virus genes: application to the reassortment of equine influenza virus genes. Virus Res 32: 391–399
2. Baldwin AS (1996) The NF-κB and IκB proteins: new discoveries and insights. Annu Rev Immunol 14: 649–681
3. Bergmann M, Garcia-Sastre A, Carnero E, Pehamberger H, Wolff K, Palese P, Muster T (2000) Influenza virus NS1 protein counteracts PKR-mediated inhibition of replication. J Virol 74: 6203–6206
4. Brewis N, Phelan A, Webb J, Drew J, Elliott G, O'Hare P (2000) Evaluation of VP22 spread in tissue culture. J Virol 74: 1051–1056
5. Coates DM, Sweet C, Smith H (1986) Severity of fever in influenza: differential pyrogenicity in ferrets exhibited by H1N1 and H3N2 strains of differing virulence. J Gen Virol 67: 419–425
6. Elliott G, O'Hare P (1997) Intracellular trafficking and protein delivery by a herpesvirus structural protein. Cell 88: 223–233
7. Elliott G, O'Hare P (2000) Cytoplasm-to-nucleus translocation of a herpes tegument protein during cell division. J Virol 74: 2131–2141

8. Everett H, McFadden G (1999) Apoptosis: an innate immune response to virus infection. Trends Microbiol 7: 160–165
9. Fesq H, Bacher M, Nain M, Gemsa D (1994) Programmed cell death (apoptosis) in human monocytes infected by influenza A virus. Immunobiology 190: 175–182
10. Flory E, Kunz M, Sheller C, Jassoy C, Stauber R, Rapp UR, Ludwig, S (2000) Influenza virus-induced NF-κB-dependant gene expression is mediated by overexpression of viral proteins and involves oxidative radicals and activation of IκB kinase. J Biol Chem 275: 8307–8314
11. Gill TA, Morley PJ, Sweet C (2000) Replication-defective mutants of mouse cytomegalovirus protect against wild-type virus challenge. J Med Virol 62: 127–139
12. Hatada E, Fukuda R (1992) Binding of influenza A virus NS1 protein to dsRNA in vitro. J Gen Virol 73: 3325–3329
13. Hinshaw VS, Olsen CW, Dybdahl-Sissoko N, Evans D (1994) Apoptosis: a mechanism of cell killing by influenza A and B viruses. J Virol 68: 3667–3673
14. Hogue BG, Nayak DP (1992) Synthesis and processing of the influenza virus neuraminidase, a type II transmembrane glycoprotein. Virology 188: 510–517
15. Hoffmann E, Neumann G, Kawaoka Y, Hobom G, Webster RG (2000) A DNA transfection system for generation of influenza A virus from eight plasmids. Proc Natl Acad Sci USA 97: 6108–6113
16. Kaltschmidt B, Kaltschmidt C, Hofmann TG, Hehner SP, Droge W, Schmitz ML (2000) The pro- or anti-apoptotic function of NF-κB is determined by the nature of the apoptotic stimulus. Eur J Biochem 267: 3828–3835
17. Katze JM, Lu X, Tumpey TM, Smith CB, Shaw MW, Subbarao K (2000) Molecular correlates of influenza A H5N1 virus pathogenesis in mice. J Virol 74: 10807–10810
18. Kumar S (1999) Regulation of caspase activation in apoptosis: implications in pathogenesis and treatment of disease. Clin Exp Pharmacol Phys 26: 295–303
19. Lamb RA, Krug RM (1996) Orthomyxoviridae: the viruses and their replication. In: Fields BN, Knipe DM, Howley P (eds) Fields Virology, 3rd ed. Lippincott-Raven, Philadelphia, pp 1353–1396
20. Lowy RJ, Dimitrov DS (1995) Induction of apoptosis in J774.1 macrophages by influenza-virus. Mol Biol Cell 6: 2063
21. Lu Y, Wambach M, Katze MG, Krug RM (1995) Binding of the influenza virus NS1 protein to double stranded RNA inhibits the activation of the protein kinase that phosphorylates the elF-2 translation initiation factor. Virology 214: 222–228
22. Marion RM, Aragon T, Beloso A, Nieto A, Ortin J (1997) The N-terminal half of the influenza virus NS1 protein is sufficient for nuclear retention of mRNA and enhancement of viral mRNA translation. Nucleic Acids Res 25: 4271–4277
23. Massague J (1990) The transforming growth factor-β family. Annu Rev Cell Biol 6: 597–641
24. Mohsin MA, Morris SJ, Smith H, Sweet C (2002) Correlation between levels of apoptosis, levels of infection and haemagglutinin receptor binding affinity of various subtypes of influenza virus: does the viral neuraminidase have a role in these associations. Virus Res in press
25. Mori I, Komatsu T, Takeuchi K, Nakak U, Ki K, Sudo M, Kimura Y (1995) In vivo induction of apoptosis by influenza virus. J Gen Virol 76: 2869–2873
26. Morris SJ, Price GE, Barnett JM, Hiscox SA, Smith H, Sweet C (1999) Role of neuraminidase in influenza virus-induced apoptosis. J Gen Virol 80: 137–146
27. Nilsen EM, Johansen F-E, Jahnsen FL, Lundin KEA, Scholz T, Brandtzaeg P, Haraldsen G (1998) Cytokine profiles of cultured microvascular endothelial cells from the human intestine. Gut 42: 635–642

28. Oh S, McCaffery JM, Eichelberger MC (2000) Dose-dependent changes in influenza virus-infected dendritic cells result in increased allogenic T-cell proliferation at low, but not high, doses of virus. J Virol 74: 5460–5469
29. Phelan A, Elliott G, O'Hare P (1998) Intercellular delivery of functional p53 by the herpesvirus protein VP22. Nature Biotechn 16: 440–443
30. Price GE, Fenton RJ, Smith H, Sweet C (1997) Are known pyrogenic cytokines responsible for fever in influenza? J Med Virol 52: 336–340
31. Price GE, Smith H, Sweet C (1997) Differential induction of cytotoxicity and apoptosis by influenza virus strains of differing virulence. J Gen Virol 78: 2821–2829
32. Restifo NP (2000) Building better vaccines: how apoptotic cell death can induce inflammation and activate innate and adaptive immunity. Curr Opinion Immunol 12: 597–603
33. Schultz-Cherry S, Dybdahl-Sissoko N, Neumann G, Kawaoka Y, Hinshaw VS (2001) Influenza virus NS1 protein induces apoptosis in cultured cells. J Virol 75: 7875–7881
34. Schultz-Cherry S, Hinshaw VS (1996) Influenza virus neuraminidase activates latent transforming growth factor-β. J Virol 70: 8624–8629
35. Schultz-Cherry S, Krug RM, Hinshaw VS (1998) Induction of apoptosis by influenza virus. Semin Virol 8: 491–495
36. Takizawa T, Fukuda R, Miyawaki T, Ohashi K, Nakanishi Y (1995) Activation of the apoptotic Fas-antigen-encoding gene upon influenza virus infection involving spontaneously produced β-interferon. Virology 209: 288–296
37. Takizawa T, Matsukawa S, Higuchi Y, Nakamura S, Nakanishi Y, Fukuda R (1993) Induction of programmed cell death (apoptosis) by influenza virus infection in tissue culture cells. J Gen Virol 74: 2347–2355
38. Takizawa T, Ohashi K, Nakanishi Y (1996) Possible involvement of dsRNA-activated protein kinase in cell death by influenza virus infection. J Virol 70: 8128–8132
39. Takizawa T, Tatematsu C, Ohashi K, Nakanishi Y (1999) Recruitment of apoptotic cysteine proteases (caspases) in influenza virus-induced cell death. Microbiol Immunol 43: 245–252
40. Tan SL, Katze MG (1998) Biochemical and genetic evidence for complex formation between the influenza A virus NS1 protein and the interferon-induced PKR protein kinase. J Interfer Cyt Res 18: 757–766
41. Teodoro JG, Branton PE (1997) Regulation of apoptosis by viral gene products. J Virol 71: 1739–1746
42. Wada N, Matsumura M, Oba Y, Kobayashi N, Takizawa T, Nakanishi Y (1995) Transcription stimulation of the Fas-encoding gene by nuclear factor for interleukin-6 expression upon influenza virus infection. J Biol Chem 270: 18007–18012

Author's address: Dr. C. Sweet, School of Biosciences, The University of Birmingham, Edgbaston, Birmingham BIS2TT, U.K.; e-mail: c.sweet@bham.ac.uk